Buckling Behavior of Rectangular Plates with Different Central Cutouts

Mr. Ashokkumaar.A

Department of Mechanical Engineering,
Bharath institute of science and technology, Bharath University,
Chennai-600073, Tamilnadu

Abstract-

Mechanical buckling analyses were performed on rectangular plates with central cutouts. The cutouts were either circular holes or square holes. The finite-element structural analysis method was used to study the effects of plate-support conditions, plate aspect ratio, hole geometry, and hole size on the mechanical buckling strengths of the perforated plates. The compressive-buckling strengths of the plates could be increased considerably only under certain boundary conditions and aspect ratios. The plate-buckling mode can be symmetrical or antisymmetrical, depending on the plate boundary conditions, aspect ratio, and the hole size. For the same cutout areas (i.e., same plate weight density), the buckling strengths of the same-sized plates with square holes generally surpass those of the plates with circular holes over the range of hole sizes. The results and illustrations provide vital information for the efficient design of aerospace structural panels.

INTRODUCTION

In aerospace structures, cutouts are commonly used as access ports for mechanical and electrical systems, or simply to reduce weight. Structural panels with cutouts often experience compressive loads that are induced either mechanically or thermally, and can result in panel buckling. Thus, the buckling behavior of those structural panels with cutouts must be fully understood in the structural design. For an unperforated rectangular plate of finite extent (i.e., with finite length and finite width) under uniform compression, the closed-form buckling solutions are easily obtained because the prebuckling stress field is uniform everywhere in the plate. When a finite rectangular plate is perforated with a central cutout (e.g., a circular or square hole), however, the buckling analysis becomes extremely cumbersome because the cutout introduces a load-free boundary that causes the stress field in the perforated plate to be nonuniform. Hence, the closed-form buckling solutions are practically unobtainable, and various approximate methods had to be developed to analyze such perforated plates.

With the availability of powerful tools such as the well-developed, finite-element structural analysis computer programs, it is now possible to calculate the prebuckling stress fields and the buckling eigenvalue solutions quite accurately for the finite rectangular plates of any aspect ratios, containing cutouts of any geometry and any hole sizes, under any specified boundary and loading conditions.

This report investigates the mechanical- and thermal-buckling analyses of rectangular plates containing arbitrarily-sized central circular holes or square holes. A finite-element method was used to study the effects of plate aspect ratio, hole geometry, hole size, and plate boundary conditions on the mechanical and thermal-buckling strengths of perforated plates.

DESCRIPTION OF THE PROBLEM

The geometry of the perforated rectangular plates and different boundary conditions used in the finite-element analysis are described as follows.

Geometry

Figure 1 shows the geometry of two types of perforated rectangular plates with length l, width w, and thickness t. The central cutout is either a circular hole with diameter d (fig. 1(a)), or a central square hole with side c (fig. 1(b)). Table 1 lists the dimensions of various perforated rectangular plates analyzed.

Notice that all the plates have the same width, $w = 20$ in., and the same thickness, $t = 0.1$ in.
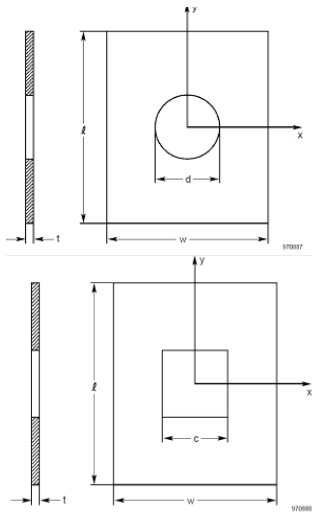
Figure 1. Rectangular plates with central cutouts.

In table 1, the range 0 ~ 0.7 covers 0, 0.05, 0.1, 0.15, 0.2, 0.25, 0.3, 0.35, 0.4, 0.45, 0.5, 0.55, 0.6, 0.65, 0.7. For a given plate aspect ratio, the 15 hole-size cases will provide 15 data points for plotting each buckling curve in the ( )cr vs. d/w (or c/w) plots. If the buckling curve has any sharp bends in certain regions, however, additional data points for d/w (or c/w) values not listed in table 1 were generated to define those sharp bend regions more accurately.

Table 1. Dimensions of perforated plates.

w, in.	t, in.	l/w	d/w	c/w
20	0.1	1.0	0 ~ 0.7	0 ~ 0.7
20	0.1	1.5	0 ~ 0.7	0 ~ 0.7
20	0.1	2.0	0 ~ 0.7	0 ~ 0.7

Boundary Conditions

The various boundary conditions considered in the mechanical- and thermal-buckling analyses are described as follows. For mechanical buckling (uniaxial compressive buckling), the four edges of the perforated plates are either simply supported or clamped. The lower edge of the plate is kept stationary and the upper edge is allowed to move freely in the loading direction (*y*-direction). The two unloaded edges are either constrained from the transverse in-plane motions. The four cases of boundary conditions considered in the analysis are as follows:

1. four edges simply supported; the two side edges can slide freely along the lubricated fixed guides.

2. four edges simply supported; the two side edges can slide freely along the lubricated

guides, which can have free in-plane transverse motions.

3. four edges clamped; the two side edges can slide freely along the lubricated fixed clamping guides .

4. four edges clamped; the two side edges can slide freely along the lubricated clamping guides, which can have free in-plane transverse motions .

FINITE-ELEMENT ANALYSIS

In the finite-element analysis, the structural performance and resizing (SPAR) finite-element computer program was used. Because of symmetry, only one quarter of the perforated plates were modeled. The plates with circular holes were modeled with both triangular combined membrane and bending elements (E33 elements) and quadrilateral combined membrane and bending elements .For the plates with square holes, only the square-shaped E43 elements were used. Two typical quarter-panel finite-element models generated for a typical circular cutout case (l/w = 1.5; d/w = 0.2) and a typical square cutout case (l/w = 1.5; c/w = 0.2) are shown, respectively,

The material properties used in the finite-element analysis are those of monolithic Ti-6Al-4V titanium alloy (ref. 15), listed in table 3.

- ○ Youngs modulus E = 1.095×10^{11} N/m^2
- ○ Shear modulus G = 0.424×10^{11} N/m^2
- ○ Poission ratio γ = 0.31

RESULTS

The following sections present the results of the finite-element mechanical- and thermal-buckling analysis of rectangular plates with circular and square holes.

Solution Accuracy

For checking the finite-element solution accuracy, the finite-element buckling solutions for simply supported solid plates (no holes) of different aspect ratios under uniaxial compression were compared with the corresponding classical buckling solutions given by Timoshenko,{1961},Theory Of Elasticity, 2nd Edition, McGraw-Hill Book. From His Theory, the critical buckling load is given by

$$N_{cr} = k\pi^2 E t^2 / 12w(1 - \upsilon^2) \qquad (1)$$

Here k is the numerical factor depends on the plate aspect ratio and boundary conditions. The following table shows the results of buckling strengths for the first boundary condition by theoretical and finite element method.

l/w ratio	k	N_{cr} (N) (Theoritical)	N_{cr} (N) (Ansys)	Error
1	4	21521.176	20386	5.2
1.5	4.66	25072.170	24466	2.4
2	3.97	21346.170	20640	3.3

Comparison of Buckling Strengths

The buckling strengths of the plates with circular holes will be compared with those of the plates with square holes under the same weight density conditions. Therefore, for a given aspect ratio of the perforated plates (no change in width *w*), the area of the square hole was set equal to that of the circular hole by adjusting the side *c* of the square hole according to the relationship.

$$c/d = \pi/2 \qquad (2)$$

Thus, before the comparison of buckling strengths could be made, the abscissa *c/w* of figures 29, 31,33, 35, 37, 39, 41, 43, and 45 must first be converted to the equivalent *d/w* using equation (2). Namely, the data points for the square hole cases must be shifted slightly toward the right because the equivalent *d/w* is slightly greater than *c/w* in view of equation (2).
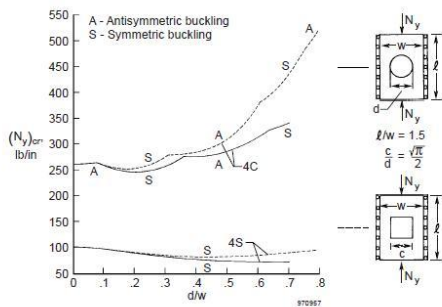

Figure 3 Comparison of compressive buckling strengths of rectangular plates with different geometrical cutouts; fixed edges.

(Fig 2-4)compare the compressive buckling strengths of the two types of perforated plates under 4S fixed and 4C fixed conditions.
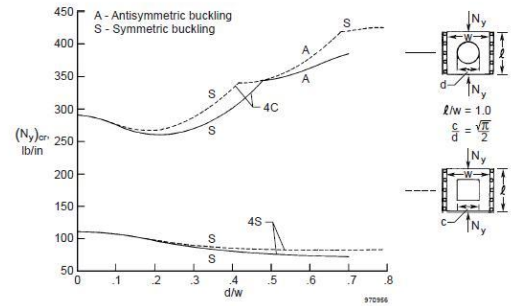

Figure 2 Comparison of compressive buckling strengths of square plates with different geometrical cutouts; fixed edges.
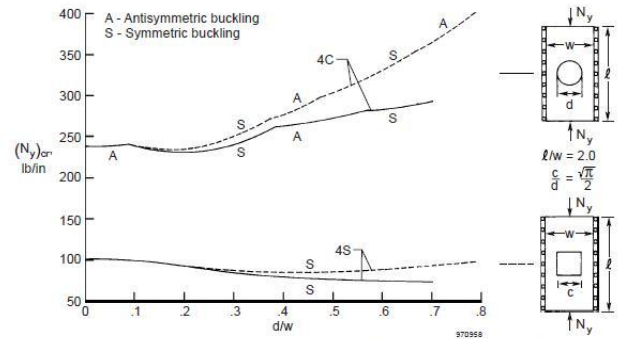

Figure 4 Comparison of compressive buckling strengths of rectangular plates with different geometrical cutouts; fixed edges.

At large hole sizes, the square hole cases exhibit higher buckling strengths than the respective circular hole case.

For the 4S free and 4C free boundary conditions, the square plates with square holes (fig.5) have higher compressive buckling strengths than those with circular holes. For the perforated rectangular plates (figs.6), the square hole cases give slightly higher buckling strengths at moderate hole sizes than the circular hole cases.
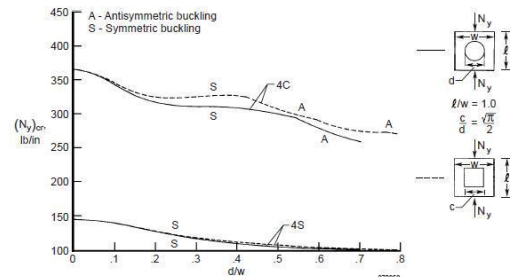

Figure 5 Comparison of compressive buckling strengths of square plates with different geometrical cutouts; free edges.

For the 4S free and 4C free boundary conditions, the square plates with square holes (fig.5) have

higher compressive buckling strengths than those with circular holes. For the perforated rectangular plates (figs.6), the square hole cases give slightly higher buckling strengths at moderate hole sizes than the circular hole cases. The reverse is true, however, for hole sizes greater than $d/w = 0.5$.
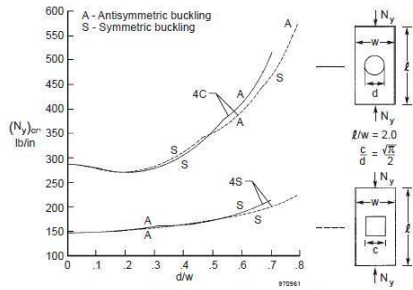

Figure 6 Comparison of compressive buckling strengths of rectangular plates with different geometrical cutouts; free edges.

DISCUSSION

The buckling behavior of plates with central holes as presented is quite peculiar because, under certain boundary conditions (especially cases with clamped edges) and plate aspect ratios, the mechanical buckling strengths of the perforated plates, contrary to expectation, increase rather than decrease as the hole sizes grow larger. The conventional wisdom is that, as the hole sizes increase, the plates lose more materials and become weaker. Therefore, the buckling strengths were expected to decrease as the hole sizes increase. This was not the case. Such peculiar buckling phenomenon of the perforated plates may be explained as follows.

When the hole size becomes considerably large relative to the plate width, most of the compressive load is carried by the narrow side strips of material along the plate boundaries. As is well known, a stronger plate boundary condition (e.g., clamped rather than simply-supported boundaries) increases the buckling strength, while the higher stress concentration decreases the buckling strength. Thus, which effects become dominant will determine the increase or decrease of the buckling strengths of the perforated plates.

For the square-hole cases, the load-carrying narrow side strips along the plate boundaries are practically under uniform compressive stress fields. For the circular-hole cases, the narrow compressed side strips are under stress concentration, which reduces the buckling strengths. This fact may explain why, for most of the cases studied (except figs. 51 and 52), the buckling strengths of the plates with square holes increase more at larger hole sizes than

the plates with circular holes having the same weight density.

The unusual buckling characteristics of the perforated plates offer vital applications in aerospace structural panel design. Namely, by opening holes of proper sizes in aerostructural panels for weight saving, their buckling strengths can be boosted simultaneously. Thus, with a single stone, one can shoot down two birds.

CONCLUDING REMARKS

Finite-element mechanical- and thermal-buckling analyses were performed on plates containing centrally located circular and square holes. The effects of plate aspect ratio, hole geometry, hole size, and plate support conditions on the mechanical- and thermal-buckling strengths and buckling mode shapes were studied in great detail. The key findings of the analysis are as follows:

• The buckling mode shapes of the perforated plates can be symmetrical or antisymmetrical depending on the hole sizes, plate aspect ratios, and plate boundary conditions.
• Increasing the hole size does not necessarily reduce the mechanical- and thermal-buckling strengths of the perforated plates. For certain plate aspect ratios and plate support conditions, mechanical- and thermal-buckling strengths increase with the increasing hole sizes.
For most cases under the same weight density conditions, the mechanical- and thermal-buckling strengths of the plates with square holes are slightly higher than those of the corresponding plates with circular holes at increasing hole sizes.
• The clamped boundary conditions more effectively enhance the mechanical- and thermalbuckling strengths of the perforated plates at larger hole sizes than the simply-supported boundary conditions.

REFERENCES

[1] Levy, Samuel, Ruth M. Woolley, and Wilhelmina D. Kroll, "Instability of Simply Supported Square Plate With Reinforced Circular Hole in Edge Compression," *Journal of Research*, National Bureau of Standards, vol. 39, research paper no. RP1849, Dec. 1947, pp. 571–577.
[2] Kumai, Toyoji, "Elastic Stability of the Square Plate With a Central Circular Hole Under Edge Thrust," *Proc. Japan Nat. Cong. Appl. Mech*., 1951, pp. 81–88.
[3] Schlack, A. L., Jr., "Elastic Stability of Pierced Square Plates," *Experimental Mechanics*, June 1964, pp. 167–172.
[4] Schlack, Alois L., Jr., "Experimental Critical Loads for Perforated Square Plates," *Experimental Mechanics*, Feb. 1968, pp. 69–74.
[5] Kawai, T. and H. Ohtsubo, "A Method of Solution for the Complicated Buckling Problems of Elastic Plates With

Combined Use of Rayleigh-Ritz's Procedure in the Finite Element Method," AFFDLTR- 68-150, 1968.

[6] Yu, Wei-Wen and Charles S. Davis, "Cold-Formed Steel Members With Perforated Elements," *J. Structural Division*, ASCE, vol. 99, no. ST10, Oct. 1973, pp. 2061–2077.

[7] Ritchie, D. and J. Rhodes, "Buckling and Post-Buckling Behaviour of Plates With Holes," *Aeronautical Quarterly*, vol. 26, Nov. 1975, pp. 281–296.

[8] Nemeth, Michael Paul, "Buckling Behavior of Orthotropic Composite Plates With Centrally Located Cutouts," Ph. D. Dissertation, Virginia Polytechnic Institute and State University, May 1983.

[9] Nemeth, Michael P., *A Buckling Analysis for Rectangular Orthotropic Plates With Centrally Located Cutouts*, NASA TM-86263, Dec. 1984.

[10] Nemeth, Michael P., Manuel Stein, and Eric R. Johnson, *An Approximate Buckling Analysis for Rectangular Orthotropic Plates With Centrally Located Cutouts*, NASA TP-2528, Feb. 1986.

[11] Nemeth, M. P., "Buckling Behavior of Compression-Loaded Symmetrically Laminated Angle-Ply Plates With Holes," *AIAA Journal*, vol. 26, no. 3, Mar. 1988, pp. 330–336.

[12] Lee, Y. J., H. J. Lin, and C. C. Lin, "A Study on the Buckling Behavior of an Orthotropic Square Plate With a Central Circular Hole," *Composite Structures*, vol. 13, no. 3, 1989, pp.173–188.

[13] Timoshenko, Stephen P. and James M. Gere, *Theory of Elastic Stability*, 2nd ed., McGraw-Hill Book Company, New York, 1961.

[14] Whetstone, W. D., *SPAR Structural Analysis System Reference Manual: System Level 13A, vol. 1, Program Execution*, NASA CR-158970-1, Dec. 1978.